Grain and crystal texture properties of absorber layers in MOCVD-grown CdTe/CdS solar cells

G Zoppi[1†], K Durose[1*], S J C Irvine[2] and V Barrioz[2]

[1] Department of Physics, University of Durham, South Road, Durham DH1 3LE, UK

[2] Department of Chemistry, University of Wales, Bangor, Gwynedd LL57 2UW, UK

Keywords: CdTe solar cells, MOCVD, $CdCl_2$ treatment, recrystallisation

Short title: Grains and crystal texture in MOCVD-grown CdTe solar cells

[†] Now at NPAC, Ellison Building, Ellison Place, Northumbria University, Newcastle upon Tyne, NE1 8ST, UK

**E-mail: ken.durose@durham.ac.uk*

Abstract

The microstructure of 4-13 μm thick CdTe absorber layers in CdTe/CdS/ITO/glass solar cell structures grown by metal-organic chemical vapour deposition (MOCVD) at 350°C has been studied. The crystalline texture, lattice parameter, and grain size were measured as a function of thickness for the as-grown layers, and as a function of annealing temperature and time for annealing in both nitrogen (N_2) and cadmium chloride ($CdCl_2$) environments. The average grain sizes developed with thickness as r (μm) = 0.050x - 0.10 ($4 < x < 12$ μm), and this behaviour is contrasted with that for close-spaced sublimation material grown at 500°C. Annealing in both ambients promoted grain growth (with Rayleigh grain size distribution functions and Burke-Turnbull exponents being $n = 7$ at 440°C and ~4 at 400°C), a development of the grown-in preferred orientation from [111] to [211], and relief of the grown-in compressive stress. A growth mechanism by which development of the [211] preferred orientation may accompany grain growth is described. It is concluded that MOCVD growth at temperatures higher than the 350°C used here will be required to produce the larger grain sizes required for photovoltaic applications.

1. Introduction

Most of the literature on CdTe solar cells concerns material grown by close-spaced sublimation (CSS), physical vapour deposition (PVD), electrodeposition (ED), or else sputtering, but there is by comparison little on metal-organic vapour phase deposited MOCVD-grown material. This is perhaps surprising since MOCVD provides an opportunity for inclusion of intentional impurity doping whereas the more commonly used routes rely on the so-called cadmium chloride ($CdCl_2$) post-growth processing

route. This is itself one of the key steps in CdTe/CdS device fabrication. Annealing with exposure to $CdCl_2$ causes conductivity type conversion of the CdTe solar absorber, passivates the grain boundaries and reduces recombination in the devices [1-4]. Indeed there are reports of the effect of post-growth treatment on the structure and performance of cells grown by for example PVD, CSS and ED [5-7]. Such treatment is known to influence recrystallisation and the preferred orientation of the films [7]. This work extends the range of knowledge for the texture, strain and grain size of MOCVD-grown films, both before and after post-growth treatment. It is a first study of such effects in relatively thick (4-13μm) MOCVD CdTe films on CdS layers.

2. Experimental details

CdTe/CdS solar cell structures were grown by MOCVD [8] on indium tin oxide/glass (ITO/glass) substrates supplied by Merck Display Technology. Substrates were cleaved into 35×50 mm pieces and cleaned using the process described in [9] prior to growth. Three substrates at a time were placed on the graphite susceptor as shown in figure 1. The substrate positions are defined as *inlet, centre* and *outlet* positions with reference to the entry and exhaust sides of the reactor tube. The CdS window layers were grown at a temperature of 300°C in a total gas flow of 3355 sccm. The saturated vapour pressures and flows of hydrogen gas carrying the organometallics were as follows: ditertiarybutylsulphide (DTBS) 2 Torr/551 sccm and dimethylcadmium (DMCd) 8 Torr/101 sccm. These values correspond to an organometallic partial pressure ratio of 1.25 (VI/II ratio) diluted in hydrogen. The final thicknesses were estimated at the centre position from interferometry [10] and were 120, 240 and 500 nm for three growth runs described here. The CdTe absorber layers were grown at 350°C on top of the CdS using

a DMCd 8 Torr/101 sccm and di-isopropyltelluride (DIPTe) 1.6 Torr/500 sccm (VI/II = 1) diluted with 2755 sccm of H_2. The monitored thickness of the CdTe layer deduced from the *in situ* laser interferometry was 8 μm and further local measurements were performed using a Tencor Instruments Alpha Step 200 stylus profiler.

Samples grown on substrates positioned at the *centre* and *inlet* positions were annealed in nitrogen (N_2) in a tube furnace over the temperature range of 360-500°C for 5-70 min. Prior to annealing, samples originating from the *centre* position were coated with a ~90 nm layer of $CdCl_2$. Specimens were characterised by means of x-ray diffraction (XRD) and scanning electron microscopy (SEM). XRD and SEM were performed using a Siemens D5000 diffractometer using the CuKα line (1.5406 Å) and using a JEOL IC-848 SEM. CdTe grain size analysis was from secondary electrons micrographs. The shape of the grains were marked on a transparency film, scanned and analysed using PC-Image 2.0 software from Foster Findlay Associates Ltd. PC-Image allows the determination of the area of every object allowing the radius of the grains to be calculated assuming a circular grain shape. XRD pattern peak determination and phase identification were accomplished using the DIFFRAC^{plus} software suite from Bruker AXS [11].

3. Results

3.1. As-grown samples

First we describe the results for the as-deposited layers. Great variations in CdTe thickness were measured depending on the substrate position, the measurements being done by stylus profilometry of the grown layers. The thickness of 8 μm deduced from

laser interferometry was confirmed for the *centre* samples which were in the range 8.5 to 9.5 μm. The *inlet* samples were thicker than expected (~12 - 13 μm) while the *outlet* ones were much thinner, ~4 μm. Thickness variation within the same sample was also observed with best uniformity measured for the *inlet* samples at ~1.5%, variations of 15% being measured for the *centre* and 40% for the *outlet* ones. These variations within the same substrate and as a function of the substrate position reflect a change in the growth rate which was estimated from the thickness measurements and is plotted in figure 2. The growth rate increases approximately exponentially as the substrate is moved closer to the reactor gas inlet and seems to reach an upper limit.

Generally, non-uniform growth is considered to be caused by either thermal and/or gaseous effects. Berrigan *et al.* for example, report the growth rate for MOCVD-grown CdTe as a function of temperature [12]. Measurements using tin globules indicate the temperature variation along the reactor to be small, and in any case, growth profiles caused by temperature profiles generally show a peak at the centre of the susceptor (its hottest position); this is not the case in figure 2. In the present case therefore, the thickness profile represents depletion of the precursor stream as it flows down the reactor, as is discussed further in section 4. For the purposes of what follows it can therefore be assumed that the properties of the films measured are as a function of thickness and not the growth temperature.

While both the CdTe and the grain size might be expected to be influenced by the underlying CdS, no evidence of systematic influence was revealed in this study. The fourteen samples reported in the texture analysis of figure. 3 (see below) for example

were drawn from growth runs with three CdS thicknesses (120, 240 and 500 nm) i.e. four or five samples from each, and each having different CdTe thickness. The dominant effects discussed in the remainder of this section could be associated with the CdTe thickness only – the effects expected from the CdS thickness might only be revealed by larger and more specifically targeted sample sets.

In order to quantify the effects of the CdTe thickness on the texture and preferred orientation of the samples, the texture coefficients C_{hkl} [7] were studied where:

$$C_{hkl} = \frac{\frac{I_{hkl}}{I_{r,hkl}}}{\frac{1}{n}\sum_{n}\frac{I_{hkl}}{I_{r,hkl}}} \quad (1)$$

and n is the number of reflections, I_{hkl} the intensity of the hkl reflection and $I_{r,hkl}$ the intensity of the hkl reflection for a completely random sample. Hence C_{hkl} gives a measure of the enhancement of the hkl reflection in comparison to a completely randomly oriented sample. The preferred orientation of each film, as a whole, was analysed from the standard deviation σ of all C_{hkl} values as compared with randomly oriented samples as:

$$\sigma = \sqrt{\sum \frac{1}{n}\left(C_{hkl} - 1\right)^2} \quad (2)$$

σ values are used to compare the degree of orientation between different samples, so that lower σ values indicate more randomly oriented samples. By way of an example the cases of randomness and complete alignment are considered for diffraction patterns containing 9 peaks (n = 9), as was indeed the case in the present work. For complete randomness, all peaks have the intensities expected for a powder and the texture coefficient C_{hkl} = 1 for all peaks hkl. The standard deviation of the texture coefficients is

zero i.e. $\sigma = 0$. For the case of complete alignment, one set of planes *hkl* scatters into the detector with non-zero intensity, and the other eight, zero intensity. C_{hkl} = 9 for the oriented planes and is zero for the other eight, with σ = 2.8. Hence both the texture coefficient and standard deviation values are a function of the number of peaks recorded.

The variations of σ and C_{hkl} as a function of the CdTe absorber layer thickness are plotted in figure 3. The dashed lines correspond to the values of σ = 2.8 and C_{hkl} = 9 expected for a completely oriented sample. Although the first nine reflections were used in the analysis, only data for the (111) and (422) planes is shown in the figure, since these are the only orientations for which $C_{hkl} > 1.5$.

For the preferred orientation work, the most important finding was that the [111] preferred orientation dominated for CdTe layers of all thicknesses. Indeed it was *most* dominant for the thinner layers (4-6 μm) for which σ = 2.5-2.7 and C_{111} = 7.9-8.5 i.e. the layers were almost fully oriented, the sum of the remaining eight C_{hkl} values being in the range 0.5-1.1. As the thickness of the layers was increased, the most dominant preferred orientation remained [111], and C_{111} did not fall below 4.0 even for the thickest layers grown (13 μm). However, the standard deviation of the texture coefficient values decreased to σ = 1.3, this being consistent with the other C_{hkl} values increasing their near-zero values recorded for thinner layers. The second strongest orientation selected, and the only other significant one, was [422] (i.e. parallel to [211]), this having C_{422} = 1.8 for thick layers as compared to 0.4 in thin ones. In summary, the as-grown films have a preferred orientation which is a function of the layer thickness.

While [111] dominates almost completely for thin layers, and is the strongest orientation for all, thicker layers become slightly randomised with the next most important orientation being [422].

The crystallite sizes at the surface of the absorber layer were estimated from secondary electron micrographs for the three different substrate positions. It was found that the grain size increases with the thickness of CdTe material. The absorber layer grown on the *outlet* substrate had grain diameters of 0.2 μm (for 4 μm thick CdTe), while at the *centre* it was 0.7 μm (9 μm thick CdTe) and ~1 μm for a 12 μm thick layer grown at the *inlet*. In the thickness range 4 μm < x < 12 μm there is an approximately linear relationship between the grain size measured at the top surface of the absorber layer and the film thickness expressed as r (μm) = 0.050x - 0.10 where r is the grain radius. It must be noted that since the interpolation to x = 0 gives negative grain sizes the equation cannot be valid for low thicknesses. There is a precedent for this: in the case of CdTe/CdS layers grown by CSS, there is an apparently linear relation between grain size and thickness for thicknesses > 1 μm. The relation found was r (μm) = 0.107x + 1.06 for 1 < x < 9 μm [13,14]. However, this too gives a non-zero intercept (positive in this case), with the overall function being better described by a relation of the form $r(x) = kx^y + c$ where $y \approx 0.5$. In the present case however, data was not collected from thin layers. But since a negative intercept is unphysical, making a simple power law fit (for comparative purposes) can only be done by assuming that the line passes close to the origin. With this assumption, the exponent y for the fit is about 1.5 i.e. the data for MOCVD samples is superlinear, whereas it was sublinear for the CSS material. It might be inferred that grain size development during MOCVD growth is very different from that during CSS. Indeed, comparing the linear regions of both, grains at the surface of

MOCVD layers can be seen to increase in size with thickness at about half of the rate observed in CSS. These differences might tentatively be ascribed to the growth temperature, with MOCVD taking place at 350°C and CSS at about 500°C.

3.2 Heat treated samples

In this section the effect of heat treatment on structures with ~12 μm thick CdTe annealed at 360-500°C for 5-70 min is described. Figure 4 shows the variations of σ, C_{111} and C_{422} as a function of annealing time for different annealing temperatures. As with the as-grown layers, only these two orientations have significant texture coefficients. At all temperatures there is a slight loss of [111] preferred orientation after the first 20 min of annealing indicated by a decrease in C_{111} texture coefficients. For longer anneal times, σ remains constant indicating no change in the degree of preferred orientation. Instead the texture coefficients indicate that the [111] preferred orientation is progressively lost and is replaced, there being an increase in [422] texture. The strongest changes were seen in films annealed at 500°C: during the first 5-10 min of annealing the [111] preferred orientation declines sharply and there is some evidence of textural randomisation before the [422] replaces it as being dominant. Similar changes occur at both 400°C and 440°C. Annealing at 360°C, i.e. close to the growth temperature, promotes less structural rearrangement, as might be expected.

For all samples analysed, the accurate determination of the lattice parameter a was performed using the method of Taylor and Nelson [15]. The lattice parameters measured were, in all cases, larger than for a powder sample (a = 6.481 Å), suggesting

that the film is subjected to compressive stress in the plane parallel to the substrate surface (figure 5(*a*)). This stress is caused by the lattice mismatch between the CdTe and the underlying CdS film, and also the difference in their thermal expansion coefficients. However, there was a clear reduction in *a* following a 10-20 min heat treatment for all temperatures. When annealing was sustained beyond 20 min, the lattice parameter was nearly invariant for treatment temperatures below 500°C. Treatment at this temperature induced greater variations in lattice parameter, with *a* decreasing further with longer annealing times. The reduction in the lattice parameter is due to a decrease in the material strain following the heat treatment. This was confirmed by Williamson-Hall plots [16] which indicated that the internal strain for the as-grown layers (1×10^{-3} to 5×10^{-3}), was reduced to between 1×10^{-5} and 7×10^{-4} after heat treatment.

Typical examples of the surface morphologies of the as-grown and N_2 heat-treated layers are shown in the SEM micrographs in figure 6. For the as-grown films, the grains are difficult to discern from the roughness of the film. However, thermal treatment progressively reveals the grain boundaries, which are especially clear after heating in N_2 at 400°C for 20 minutes (figure 6(*b*)). However, higher temperatures and longer heating times encouraged thermal etching and evaporation from the films. For example, figure 6(*c*) (440°C, 20 min) shows more deeply (thermally) etched grain boundaries than does figure 6(*b*) (400°C, 20 min), but the grains appear to be larger. Annealing for 60 min at 440°C causes the film to begin to break up (figure 6(*c*)), while a 20 minute anneal at 500°C (figure 6(*d*)) causes inhomogeneous evaporation of the complete film thickness. The extent to which grain growth occurs is difficult to determine since the grain boundaries are not always made more distinct by the annealing in nitrogen. Figure

6 does show some evidence of grain coalescence but such effects are much clearer for $CdCl_2$ treated samples which are discussed in detail in the next section.

3.3. $CdCl_2$ treated samples

Figure 7 shows the variations of texture coefficients and preferred orientation for the samples annealed in the presence of $CdCl_2$. Figure 7(*a*) shows how the standard deviation of texture coefficients, σ, decreases with annealing indicating that the films are becoming more texturally randomised. Examination of the texture coefficients themselves indicates that the [111] preferred orientation is progressively lost while the fractions of [422] (see figure 7(*b*)) and [311], [331], and [531] (not shown) increase. These effects become especially significant for 60 min annealings. However, the [422] preferred orientation is still favoured at higher temperatures, and this is marked by a higher C_{422} coefficient. The samples treated at 400°C had, in general, more random structure than layers treated at 440°C. This is consistent with the higher temperature processing favouring the [422] direction as described in the previous section.

Variations of lattice parameter with annealing time are shown in figure 5(*b*). The lattice parameter initially increases for short annealing times and then reduces for longer ones. These variations in lattice parameter indicate increased compressive stress following the first 10-20 min of annealing while for longer annealing times this stress is released. Stress calculations [17] for the present data showed that during the post-deposition thermal treatment, the stress falls from ~ -1.1×10^4 to -5.8×10^3 N.cm^{-2}. These values are larger than the critical value of formation of structural defects for CdTe (~10^3 N.cm^{-2} [18]) and therefore the formation of dislocations is anticipated [13, 19, 20].

Figure 8 shows the SEM images and grain size distributions for $CdCl_2$ treated samples annealed at 400 and 440°C for 30 min. These $CdCl_2$ treated layers comprise continuous films with grains having well defined boundaries. Longer annealing times (> 60 min) at 440°C caused the onset of inhomogeneous evaporation similar to that in figure 6(*d*). The grain size distributions were fitted using a Rayleigh distribution model which has previously been demonstrated by Cousins *et al.* [14] to describe the grain size distribution of CSS-grown CdTe/CdS solar cells as it gave closer fits than other grain size distribution functions. Grain size data from other samples was generated in the same way as shown in figure 8 in order to generate points on the graphs of mean grain size versus annealing time and temperature shown in figure 9(*a*). For all annealing times it was observed that the mean grain size was greater for the higher temperature processing. A 35-55% difference in grain size was measured between grains annealed for times up to 60 min at 400 and 440°C. It was also noted that the distribution of grain sizes becomes wider as the annealing temperature increases (figure 8). Figure 9(*a*) shows that while grain growth occurs during the first 30 min of annealing as expected, the grain size is reduced for a 60 min anneal. This observation may well be an artefact in the apparent grain sizes caused by significant inhomogeneous evaporation from the films. The time and temperature dependent grain growth observed in the initial stages of annealing were evaluated using the parabolic grain growth law described by Burke and Turnbull [21]:

$$\left(D^2 - D_0^2\right)^{1/2} = Kt^{1/n} \qquad (3)$$

where D_0 and D are the average grain sizes before and after annealing, t the annealing time, K is a constant and n the grain growth exponent. Values of n are usually greater

than 2 and only approach 2 for very pure metals – this is the 'parabolic grain growth' law. The logarithmic plot of $\left(D^2 - D_0^2\right)^{1/2}$ as function of *t* is shown in figure 9(*b*) and provides a useful reference for the reliability of grain growth measurements. The plots give linear slopes for annealing times up to 30 min and the best fit line was used to determine the grain growth exponent for the two annealing temperatures. It was found that $n = 7$ for treatment at 440°C and $n \sim 4$ at 400°C.

4. Discussion

The variation of the growth rate on the susceptor with position (figure 2) was consistent with the effects of gas phase precursor depletion during the growth of the CdTe layers. At 350°C the reaction of the precursors is known to take place by i) the formation of methyl radicals from the dimethyl cadmium, and then ii) the reaction of the methyl radicals with the diisopropyl telluride. Since the VI/II ratio was near unity it might be expected that there will be no chemical imbalance. Moroever, since the phase field of CdTe is very narrow, the compositional difference between the layers grown on different parts of the susceptor (if present) are expected to be very small indeed and unmeasurable using conventional analytical methods. It has been inferred that the effects of temperature are minimal (section 3.1). It is on this basis that the variations of structural effects with thickness are considered to be due to thickness itself rather than to some confounding variable.

For the as-grown samples there is a relationship between preferred orientation and the layer thickness, with thin layers being [111] oriented, this giving way to more randomised texture as the layers thicken. The most dominant of emerging orientation

was [422], as highlighted in figure 3 and described in section 3.1. Further to this for the as-grown films, the crystallite size of the CdTe absorber layers were found to increase with the layer thickness. Similar results have also been reported in the case of columnar structures by several other authors for PVD-grown films [22], CSS-grown films [14] and electrodeposited films [23]. For the MOCVD films grown at 350°C, the grains increase in size with thickness at half the rate that they do in CSS material, and moreover they are smaller overall: for films of 1μm thickness the average grain size for CSS material is ~1.2 μm while that for MOCVD material is ~0.15 μm. There are many examples of the increase in grain size of grains in polycrystalline films with the thickness of the film grown, but for any given growth method, the temperature has a strong influence on the overall grain size. Hence the low temperature of MOCVD growth (~350°C compared to ~500°C for CSS) could account for the large difference in grain size with the two methods, and perhaps the difference between super- sub-linear grain growth also, although this work does not indicate a mechanism. Whatever the exact cause, the small grain size of MOCVD material makes it inferior to CSS material for solar cell applications in which grain boundaries interfere with carrier collection.

The textural and grain size development changes that are associated with the surfaces of films and which are associated with the increase in the thickness of the as-grown layers suggest that these changes may have crystallographically influenced mechanism. The two key pieces of evidence are a) that thicker films have larger grains than thinner ones and b) while both thick and thin films are dominated by the [111] preferred orientation, in the thicker films [111] is accompanied by a significant fraction of [422] oriented grains with the balance being of randomly oriented grains (the texture coefficients are

C_{111} = 4.0, C_{422} = 1.8 with the sum of the other seven reflections being 3.2). [422] may therefore be considered significant. Here, we discuss whether the [422] orientation is favoured with increasing thickness, in that lateral grain growth (i.e. in directions perpendicular to <422>, and hence <211>) may be favoured crystallographically. Planes of the <211> zones include {111} close packed planes, the Te terminated variant of {111} being the fastest growing CdTe plane of all in vapour growth experiments of orientation versus growth rate. Grain size development is considered to occur by means of competition between grains with the fastest growing faces of grains competing favourably against the slower growing faces of their neighbours. If this is the case, then grains with a [211] surface orientation will be at an advantage, since the fast growing {111} planes will be perpendicular to the film and this will favour lateral growth of such grains.

Now the response of the films to heat treatment in N_2 and to heating with $CdCl_2$ shall be discussed with reference to their lattice parameter, strain, texture and grain growth. All of these measurable parameters changed upon annealing, the changes being significant for $T \geq 400°C$ (i.e. 50°C or more than the growth temperature and above), and are accelerated for higher temperatures.

Throughout this work all the lattice parameters measured were greater than the generally accepted bulk value of 6.481 Å [24], this being the case for the as-grown and for all of the post-growth processed samples. Even for samples that had undergone heating in nitrogen, and for which the residual strain was estimated as 10^{-5}, the lattice parameter was measured to be typically 6.4865 Å. Such layers are essentially relaxed

and complete relaxation might only be expected to further reduce the lattice parameter value in the fifth significant figure. Moreover, all of the Nelson-Riley plots showed lattice parameters for each set of planes represented belonged to a single population. For a comparison the reader is referred to reference [7] in which the CdTe matrix material with [111] preferred orientation was strained with respect to other [*hkl*] orientations that belonged to recrystallised grains in the same sample i.e. the sample had grain populations with two distinct lattice parameters. In the present work the reason for this overall discrepancy in the lattice parameter is not connected to interfacial mixing at the CdTe/CdS interface – this would act to reduce the lattice parameter – and in any case, the layers are so thick (9-12 μm) that diffusion to the surface is unlikely, and the penetration of the x-rays is limited to about 2 μm. It must be considered that the lattice parameter of the films grown by MOCVD at 350°C is greater than the accepted powder value. This is possible as a result of stoichiometric variation, which can put the lattice parameter in the range $6.480 < a < 6.488$ Å as determined from melt growth experiments from Cd and Te-rich melts respectively [24]. However, the authors know of no direct confirmation from other work that the lattice parameter is consistent with Te-rich growth, but this may be because of the difficulties in measurement arising from the interfacial strain associated with thin film epitaxy.

The reduction of the lattice parameter to less than its initial value upon heating in N_2 or with $CdCl_2$ is consistent with the relief of compressive interfacial strain after long post-growth processing treatments. Nevertheless, figure 5 shows an initial increase in lattice parameter for annealing times up to about 20 minutes, and this would indicate that

compressive strain is first increased then decreased. The present experiments give no indication of the reason for this increase, but this may be the subject of future work.

In their as-grown state the texture of the layers is [111], this being usual for low temperature growth on polycrystalline CdS substrates. While increasing the thickness of the CdTe layers causes the [111] preferred orientation to be weakened, the thick layers used for annealing tests were nevertheless [111] dominated. Annealing, both with and without $CdCl_2$, caused re-arrangement of the preferred orientation. This can only happen by a) the formation of new grains which replace the old ones (recrystallisation), or b) the growth of some grains at the expense of others (grain growth). Since no second population of grains with a new lattice parameter was revealed by the x-ray diffraction work, there is no direct evidence for recrystallisation. On the other hand grain growth was observed as described in the next paragraph.

To conclude the discussion of preferred orientation, a comparison of the effects of N_2 and $CdCl_2$ annealing is made. For the N_2 annealing, the starting material was 11-12 μm thick and C_{111} was 5, (the maximum possible value was 9), this transforming into material for which the dominant orientation was [422] with C_{422} being 4. For the $CdCl_2$ annealing, the starting material was 9-10 μm thick and C_{111} was 8, (the maximum possible value was 9), this transforming into material with no dominant orientation and for which no peak had $C_{hkl} > 2.5$. Clearly the material behaves differently in each case, but the thickness, and hence texture, of the starting materials used may have influenced this. This point of detail has not been investigated further in this first study on texture in thick MOCVD films.

Finally, clear systematic evidence of grain growth is seen for the $CdCl_2$ treated films as shown in figures 8 and 9. Only films processed for the longest periods of time (60 mins) showed an apparent decrease in the average grain size. This is attributed to an artefact of feature size measurement on films from which substantial evaporation has taken place, and where the remaining particles have a size less than the maximum grain size. Indeed this break up of the films may even have contributed to the strain relief. The observation of grain growth adds weight to the argument that the textural changes associated with processing are mediated by grain growth rather than by recrystallisation, for which we have no direct evidence from the experiments in this particular study.

5. Conclusions

Structures comprising CdTe/CdS/ITO/glass layers for use in solar cells were grown with the CdTe thickness being varied between 4 and 13 μm. It is the structural properties to the CdTe layers that are the subject of this work. The crystalline texture, lattice parameter, and grain size were measured as a function of thickness for the as-grown layers and as a function of annealing temperature and time for annealing in both N_2 and $CdCl_2$ environments. Surface morphology and strain were also investigated for the annealed samples.

It is significant for the possible use of *low temperature* MOCVD CdTe films in solar cell applications that their grain size is markedly smaller than that in CdTe films grown by close-spaced sublimation (CSS). For 1 μm thick CdTe layers the grain size in MOCVD films grown at 350°C is ~0.15 μm while that for CSS material grown at 500°C is ~1.2 μm. Large grains are desirable for both solar cell performance and

stability, since the grain boundaries interfere with current transport, act as recombination centres and are pathways for diffusion. Moreover, while for most polycrystalline films the grain size develops with thickness, this occurs at half the rate in MOCVD material grown at 350°C as it does in CSS layers grown at 500°C. Furthermore, whereas for CSS-grown material the grain size develops according to a sub-linear relation (square root behaviour), it is super-linear for this MOCVD material, with the exponent being ~1.5. The texture of the films also develops with growth: thin layers are [111] oriented and become less ordered on thickening, with some favouring of the [422] orientation. Since this is associated with grain size enlargement, a crystallographic mechanism of grain growth was suggested. It is postulated that in-plane grain expansion takes place on the fast growing Te-terminated close packed planes, these being perpendicular to the film for [422] or [211] oriented growth.

Upon heating in either N_2 or $CdCl_2$, grain growth, strain relief and texture development are all observed. However, while there is no direct evidence of recrystallisation from these experiments, but it cannot be ruled out entirely for MOCVD layers. Differences in the textural development did occur between films which appeared to be influenced by the processing environment: processing transformed the [111] orientation of as-grown films to either [422] for N_2 annealing or to random texture for $CdCl_2$ annealing. However, these differences might be a function of the slight differences between the starting materials (layer textures) used in this study rather than arising from any fundamental mechanism.

For all of the layers studied in this work, and for all processing treatments applied, the lattice parameter of the CdTe was always greater than the accepted powder value of

6.481Å. Since this was true even for films with very low strain, it is suggested here that this may be a stoichiometric effect related to MOCVD growth at 350°C.

These observations give workers on CdTe/CdS solar cells an indication of the grain structures that may be expected in as-grown MOCVD layers and of the effects of annealing by the $CdCl_2$ processing that is standard in the fabrication of working cells. However it must be concluded that the small grain size obtained might best be improved upon by raising the temperature of the MOCVD growth process. This may itself require use of a Te precursor with a higher pyrolysis temperature than di-isopropyl telluride.

Acknowledgments

The authors are thankful to the EPSRC for financial support under grants GR/R21059, GR/R20816/01 and GR/S72108/01. G. Zoppi would also like to thank John Evans (Department of Chemistry, Durham University) for use of the x-ray diffraction facilities.

References

[1] T. Schulmeyer, J. Fritsche, A. Thissen, A. Klein, W. Jaegermann, M. Campo, and J. Beier, Thin Solid Films **431-432** (2003) 84-89

[2] M. Terheggen, H. Heinrich, G. Kostorz, A. Romeo, D. Baetzner, A. N. Tiwari, A. Bosio, and N. Romeo, Thin Solid Films **431-432** (2003) 262-266

[3] K. Durose, D. Boyle, A. Abken, C. J. Ottley, P. Nollet, S. Degrave, M. Burgelman, R. Wendt, J. Beier, and D. Bonnet, Physica Status Solidi a **229** (2002) 1055-1064

[4] J. Fritsche, T. Schulmeyer, A. Thi[ss]en, A. Klein, and W. Jaegermann, Thin Solid Films **431-432** (2003) 267-271

[5] A. Romeo, D. L. Batzner, H. Zogg, and A. N. Tiwari, Thin Solid Films **361-362** (2000) 420-425

[6] K. D. Rogers, J. D. Painter, D. W. Lane, and M. Healy, Journal of Electronic Materials **28** (1999) 112-117

[7] H. Moutinho, M. Al-Jassim, D. H. Levi, P. C. Dippo, and L. L. Kazmerski, Journal of Vacuum Science and Technology **A 16** (1998) 1251-1257

[8] S. J. C. Irvine, A. Hartley, and A. Stafford, Journal of Crystal Growth **221** (2000) 117-123

[9] S. J. C. Irvine, V. Barrioz, A. Stafford, and K. Durose, Thin Solid Films **480-481** (2005) 76-81

[10] A. Stafford, S. J. C. Irvine, K. L. Hess, and J. Bajaj, Semiconductor Science and Technology **13** (1998) 1407

[11] DIFFRAC^{plus}, *Software Solutions for X-ray Powder Diffraction*, (2000) Bruker AXS, Karlsrushe

[12] R. A. Berrigan, N. Maung, S. J. C. Irvine, D. J. Cole-Hamilton, and D. Ellis, Journal of Crystal Growth **195** (1998) 718-724

[13] M. A. Cousins and K. Durose, Proceedings of the 16th European Photovoltaic Solar Energy Conference, Glasgow, UK (2000) 835-838

[14] M. A. Cousins and K. Durose, Thin Solid Films **361-362** (2000) 253-257

[15] C. Barrett and T. B. Massalski, 3rd edition (1980) Pergamon press

[16] G. K. Williamson and W. H. Hall, Acta Metall. **1** (1953) 22-31

[17] B. Qi, D. Kim, D. L. Williamson, and J. U. Trefny, Journal of the Electrochemical Society **143** (1996) 517-523

[18] R. Balasubramanian and W. R. Wilcox, Materials Science and Engineering B **16** (1993) 1-7

[19] K. Durose and G. J. Russell, Journal of Crystal Growth **101** (1990) 246-250

[20] K. Durose, A. T. Fellows, A. W. Brinkman, and G. J. Russel, Journal of Materials Science **20** (1985) 3782-3789

[21] F. J. Humphreys and M. Hatherly, (1995) Pergamon

[22] B. E. McCandless, L. V. Moulton, and R. W. Birkmire, Progress in Photovoltaics: Research and Applications **5** (1997) 249-260

[23] K. D. Rogers, J. D. Painter, M. J. Healy, D. W. Lane, and M. E. Ozsan, Thin Solid Films **339** (1999) 299-304

[24} D. J. Williams 'Densities and lattice parameters of CdTe, CdZnTe and CdTeSe' in Properties of Narrow Gap Cadmium - based Compounds Ed Capper. EMIS Datareviews Series No 10 (1994) 399-402

List of Figure captions

Figure 1: Diagram showing the arrangement of the ITO/glass substrates on the graphite susceptor block for the growth of CdTe/CdS solar cell structures.

Figure 2: Estimated growth rate as a function of the substrate position. The errors originate from the uncertainty of the substrate position. Note the logarithmic scale of the growth rate axis

Figure 3: Crystal texture data as a function of thickness for as-grown CdTe layers. (a) Degree of preferred orientation σ (◊) and (b) texture coefficients C_{hkl} of the (111) (○) and (422) (△) reflections. The dashed lines indicate the values corresponding to full preferred orientations.

Figure 4: Degree of preferred orientation σ (a), texture coefficients C_{hkl} of the (111) (b) and (422) (c) reflections as function of the annealing time for different annealing temperatures. The markers are experimental data and the lines are a guide to the eye.

Figure 5: Lattice parameter as function of annealing time for heat treated samples (a) and $CdCl_2$ treated samples (b)**.** The markers are experimental data and the lines are a guide to the eye.

Figure 6: SEM micrographs of the 12 μm absorber layer surfaces of CdTe/CdS structures treated in nitrogen at different annealing temperature: (a) as-deposited, (b) 400°C for 20 min, (c) 440°C for 20 min, (d) 440°C for 60 min, (e) 500°C for 20 min. The images were recorded at 20 keV. The scale marker is identical for all images.

Figure 7: Degree of preferred orientation σ (a), texture coefficients C_{hkl} (b) for $CdCl_2$ treated samples at 400°C (dashed line) and 440°C (solid line). C_{hkl} is shown for the (111) (opened symbols) and (422) (closed symbols) reflections. The markers are experimental data and the lines are a guide to the eye.

Figure 8: SEM micrographs and grain size distributions of $CdCl_2$ treated samples annealed at (a) 400°C/30 min: mean = 0.49 μm, SD = 0.30 μm, sample = 510 grains, and (b) 440°C/30 min: mean = 0.67 μm, SD = 0.33 μm, sample = 278 grains. The scale marker is identical for both images.

Figure 9: (a) Evolution of the mean grain radii with annealing time for samples treated in $CdCl_2$ at 400°C (○) and 440°C (△) and 500°C (□). (b) Grain growth isotherms for sample treated with $CdCl_2$ at 400°C (○) and 440°C (△). The lines are the best fits for each temperature. Note that data for the 60 min annealings were not taken into account for the fits as reduced grain growth was observed for these samples compared to those annealed for 30 min.

Figure 1, Zoppi et al.

Figure 2, Zoppi et al.

Figure 3, Zoppi et al.

Figure 4, Zoppi et al.

Figure 5, Zoppi et al.

Figure 6, Zoppi et al.

Figure 7, Zoppi et al.

Figure 8, Zoppi et al.

Figure 9, Zoppi et al.

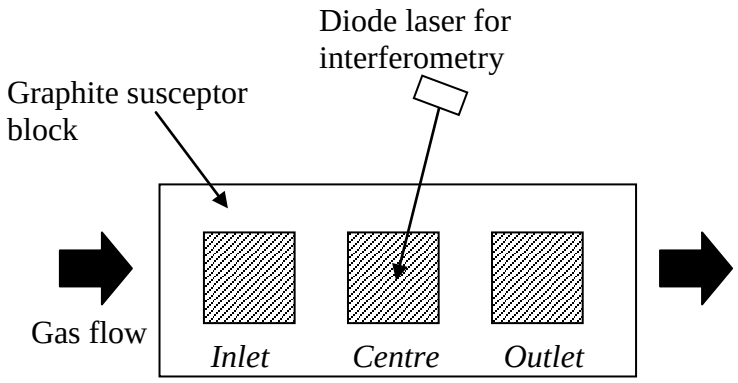

Figure 1, Zoppi et al.

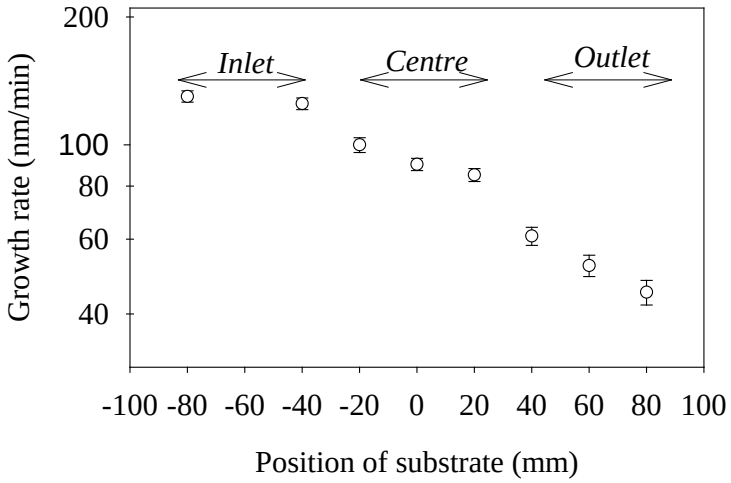

Figure 2, Zoppi et al.

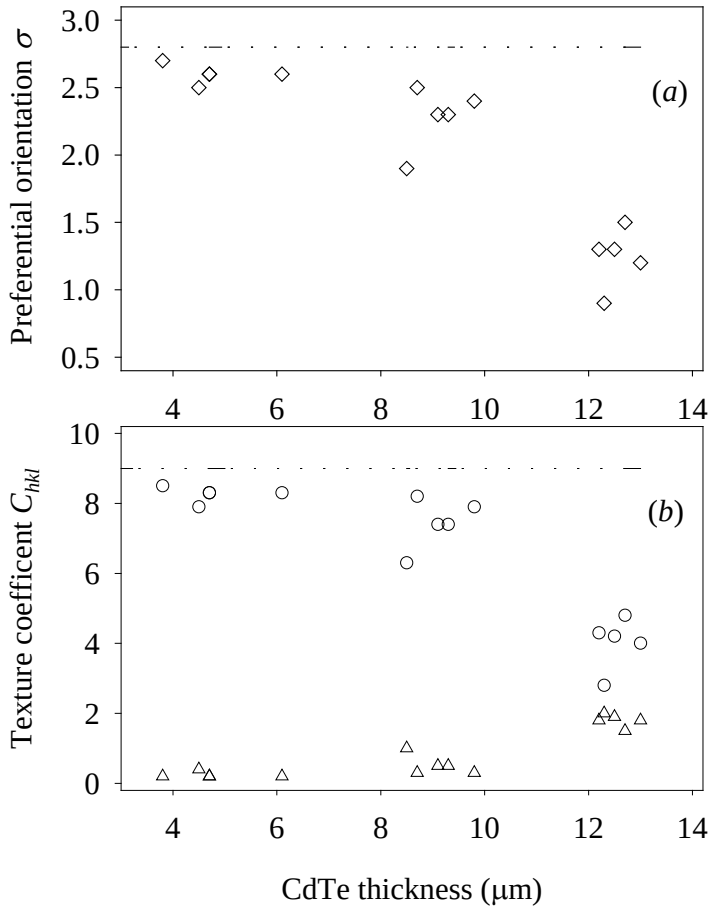

Figure 3, Zoppi et al.

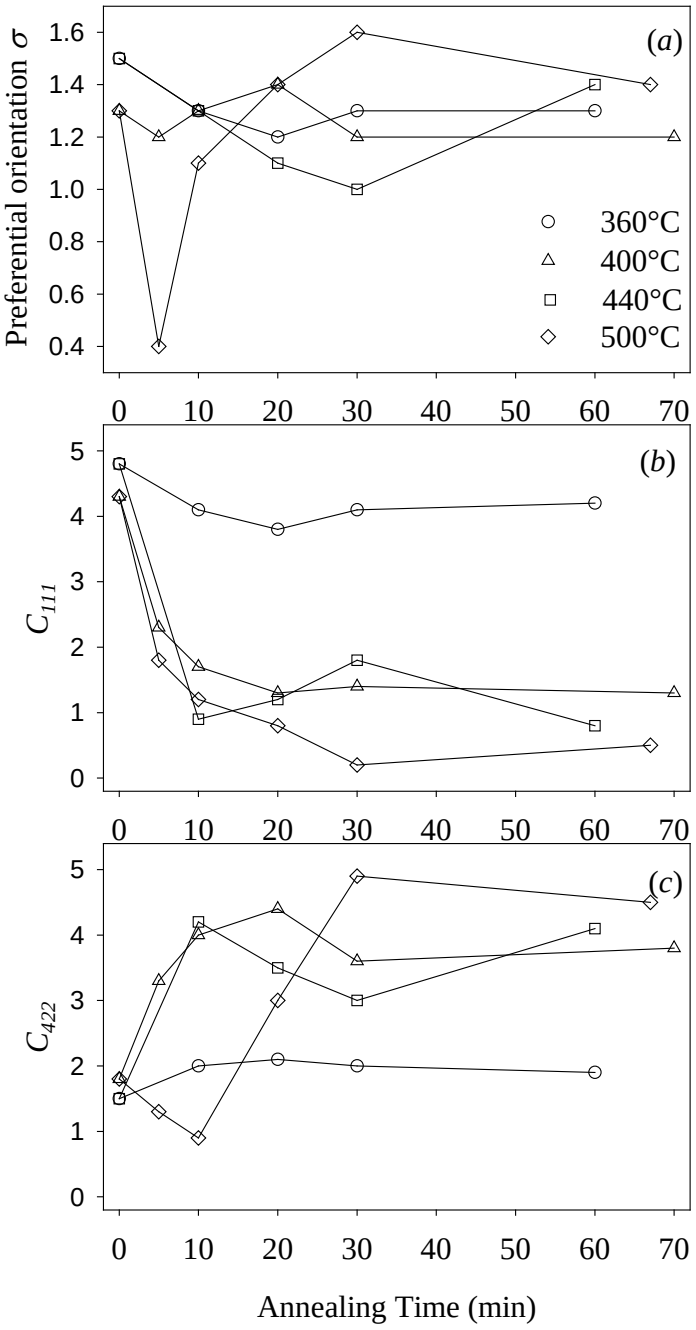

Figure 4, Zoppi et al.

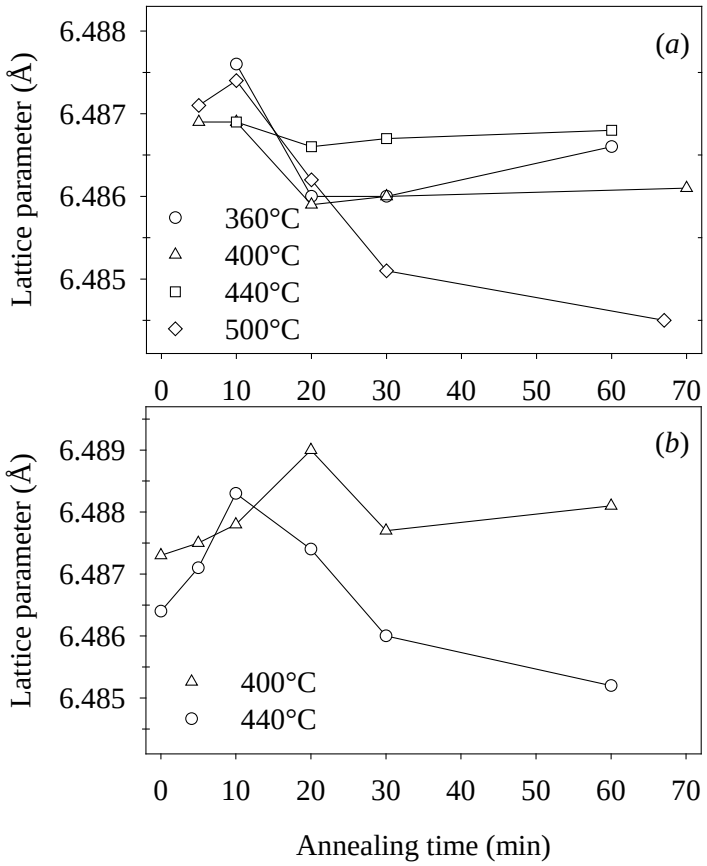

Figure 5, Zoppi et al.

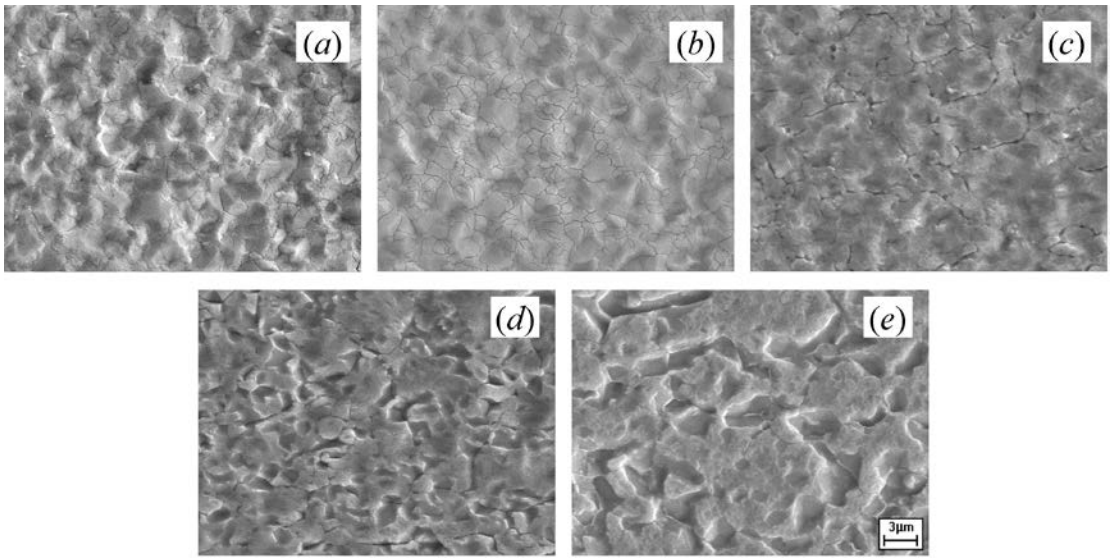

Figure 6, Zoppi et al.

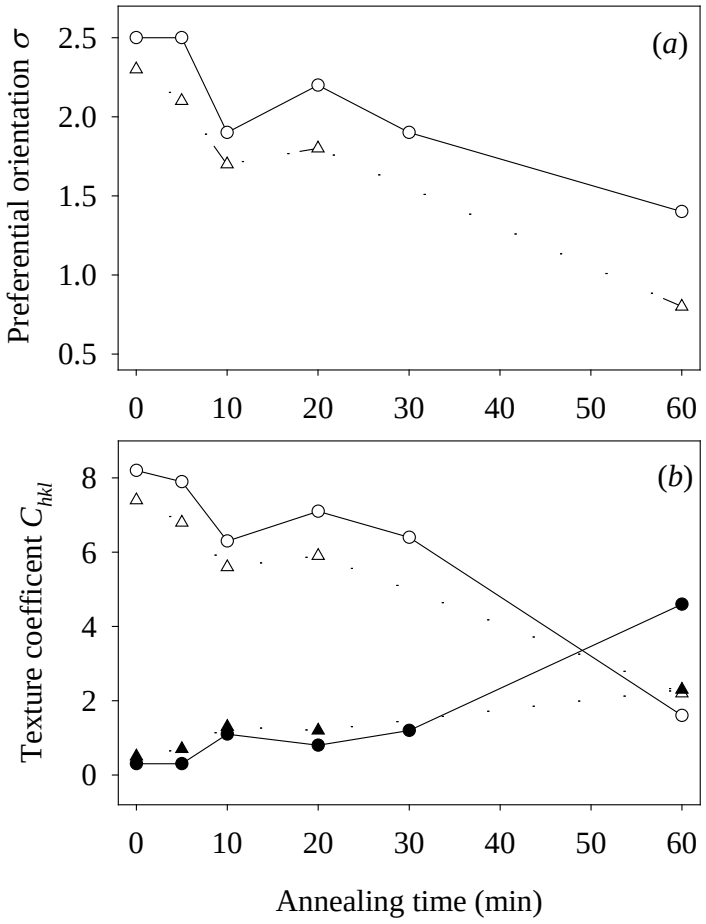

Figure 7, Zoppi et al.

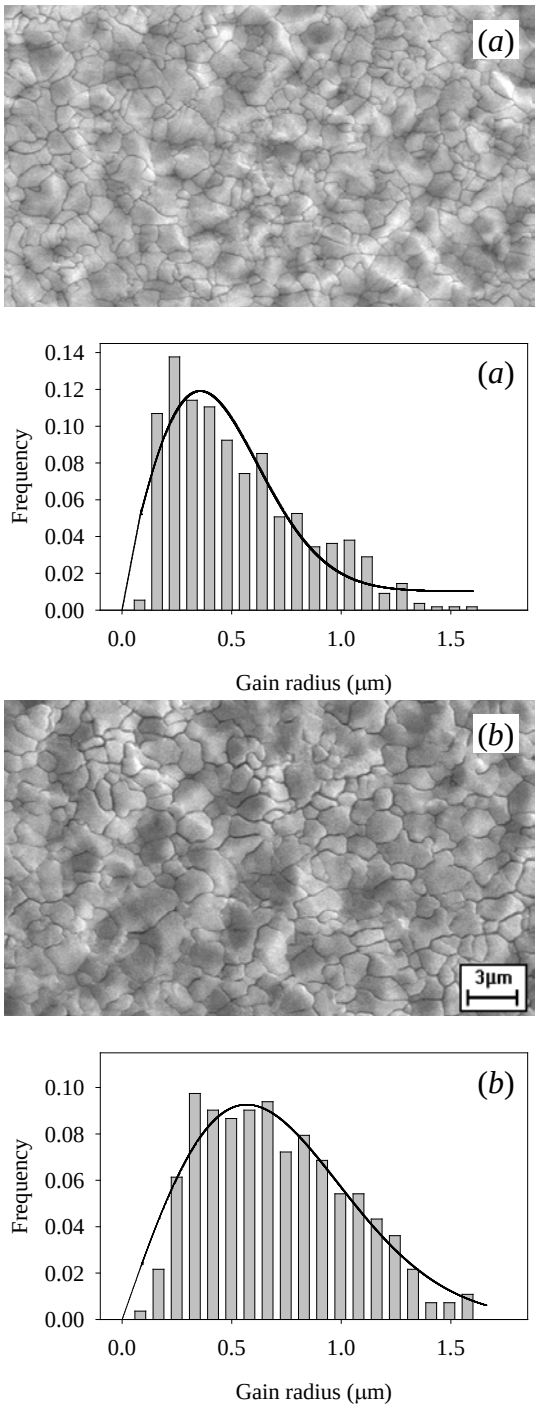

Figure 8, Zoppi et al.

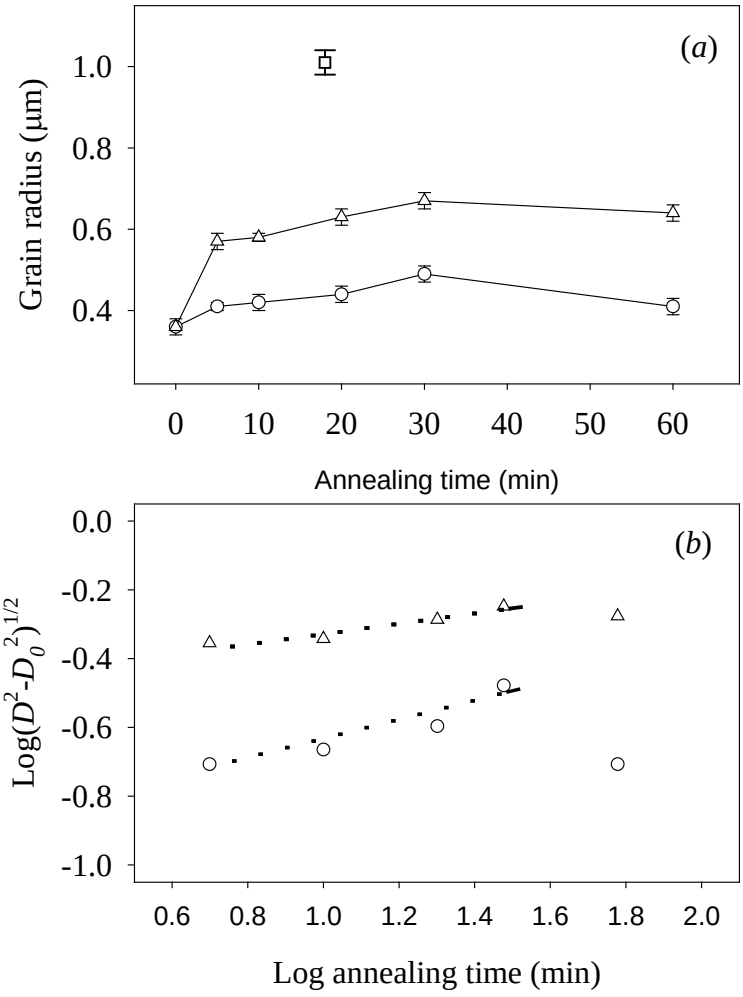

Figure 9, Zoppi et al.